Unified Model of High Step-up DC-DC Converter with Multi-cell Diode-Capacitor/Inductor Network

Yan Zhang[12], Zhuo Dong[1], Jinjun Liu[1], Yanfei Liu[2]
[1]State Key Lab of Electrical Insulation and Power Equipment, Xi'an Jiaotong University, Xi'an, Shaanxi, China
[2]Department of Electrical and Computer Engineering, Queen's University, Kingston, Canada
Email: zhangyanjtu@mail.xjtu.edu.cn

***Abstract*—Multi-cell diode-capacitor/inductor based boost derived DC-DC converter provides a simple solution for high step-up voltage regulation in solar and fuel cell generation. However, many passive components increase the order of system model and complexity. Transient modeling analysis reveals that time constant of each component in diode-capacitor/inductor network is much smaller than that of other circuit if the directly charging and discharge processes between capacitor through diode is fast enough. The voltage/current relationship of each capacitor/inductor in multi-cell network is fixed. Multi-cell diode-capacitor/inductor network can be seemed as multi-stage DC transformer. Based on the unique feature, this paper proposes the reduced-order modeling approach for high step-up DC-DC converter with multi-cell diode-capacitor/inductor network. Finally, simulation and experiments verify the correctness and effectiveness of new modeling approach. The unified reduced-order model contributes to better understanding of circuit characteristic and simplification of controller parameters design.**

Keywords—Controller design; DC-DC converter; Multi-cell diode-capacitor/inductor network; High voltage gain; Reduced-order model;

I. INTRODUCTION

Given the efficiency and environmental benefits, solar and fuel cell generation systems have rapidly developed in recent years. In photovoltaic (PV) systems, it is difficult to realize a series connection of PV cells without incurring shadow effect [1]. Fuel cell and lightweight battery power supply system are promising in future hybrid electric vehicle, more-electric aircraft and vessel. However, the obvious characteristic of these dc sources is low voltage supply. The basic DC-DC converter has encountered voltage boost limitation due to the parasitic parameters of main circuit. Therefore, high step-up voltage boost capability is the requirement of power electronic converter with wide input voltage range, high efficiency and high power density. It has been the key scientific and technical issue in above renewable energy generation [2]-[15].

High voltage gain techniques mainly includes isolated DC-DC converter with transformer, non-isolated DC-DC converter with couple inductor, multi-stages cascade structure, modular multilevel, switch-capacitor/inductor and impedance network. In which, a family of basic boost derived DC-DC converter introduces diode-capacitor/inductor network to achieve high voltage gain and avoid extreme large duty ratio. With the increasing number of basic voltage boost cell, voltage gain can be further increased. Moreover, it does not increase control circuit complexity due to only one fully controllable switch. Compared to other existing techniques, high step-up DC-DC converter with diode-capacitor/inductor network are promising in aforementioned medium and small power generation system.

Multi-cell diode-capacitor/inductor network introduces a lot of passive components which increases the order of system model. Moreover, it increases the complexity of modeling and closed-loop controller design. The typical modeling method for basic DC-DC converter is not suitable directly. Therefore, research on reduced-order modeling approach is necessary.

This paper first makes transient analysis and reveals that the time constant of diode-capacitor/inductor network is much smaller than that of other passive components. The capacitor voltage relationship among multi-cell diode-capacitor/inductor network is fixed and independent to boost duty ratio. Based on this unique feature, this paper proposes the reduced-order modeling method for this kind of high step-up DC-DC converter. Then, the unified average model and small signal transfer function are derived. Finally, simulation and experiment verify the correctness of the reduced-order model.

II. HIGH STEP-UP DC-DC CONVERTER WITH MULTI-CELL CAPACITOR/INDUCTOR NETWORK

A family of existing high step-up DC-DC converter introduces basic diode-capacitor/inductor voltage boost cell, whose network structure and future have obvious similarity. One typical network structure is shown in Fig.1. In which, *a*, *b*, *c* can be replaced with diode, capacitor or inductor. Based on this structure, Table.1 lists all the useful voltage regulation cells with symmetrical distribution of diode and passive component. According to terminal number, future and voltage regulation capability, they can be divided into two/three/four-terminal cell, voltage/current-source cell, and impedance-source cell. Where, impedance-source cell is also named as Z-source network, which is not discussed in this paper. As for other cells, capacitor voltage and inductor current direction are unique due to unilateral conduction of diode. Taking two-terminal diode-inductor network for example, two inductors charge in parallel and discharge in series. Thus, it has voltage boost capability. As for two-terminal diode-capacitor cell, it just has voltage buck capability. Appling all the voltage boost cell in basic boost DC-DC converter, the derived high step-up DC-DC converters are shown in Fig.2.

This work was supported in part by the State Key Laboratory of Electrical Insulation and Power Equipment under the Grant EIPE14112 and EIPE16310 and Power Electronics Science and Education Development Program of Delta Environmental & Educational Foundation.

With increasing number of basic diode-capacitor/inductor cells, voltage gain of boost derived DC-DC converter can be further increased. One way is to introduce multi-cell network with the same voltage-boost cells in cascade connection. And another way is to use different kinds of voltage-boost cell. However, multi-cell network with the same basic cell may have more than one extension method.

According to terminal characteristic, two-terminal diode-inductor/capacitor network can be seemed as a controlled current source, which is similar to inductor. Thus, besides the exiting multi-cell cascade extension method, each inductor in two-terminal diode-inductor/capacitor cell can be substituted by a new cell, which is called embedded extension in this paper. Fig.3 shows the possible multi-cell extension methods with cascade, embedded and hybrid connection (N=3). The different kinds of three-cell diode-inductor network have the

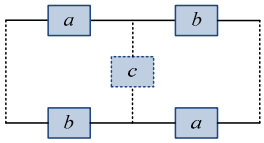

Fig.1 The symmetrical diode-capacitor/inductor network.

Table.1 Diode-capacitor/inductor voltage regulation cell

	Two-terminal cell	Three-terminal cell	Four-terminal (two-port) cell
	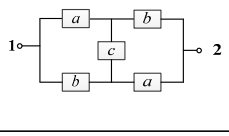	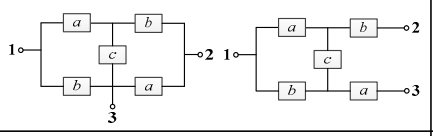	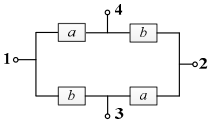
Boost cell	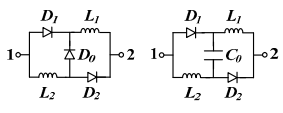	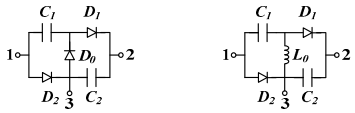	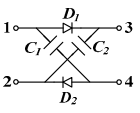
Buck cell	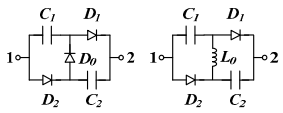	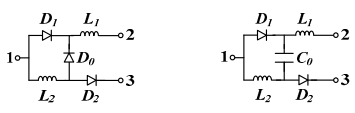	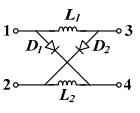
Impedance cell	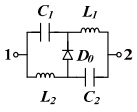	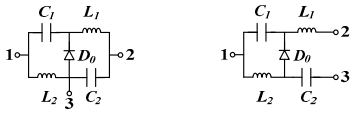	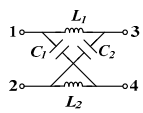

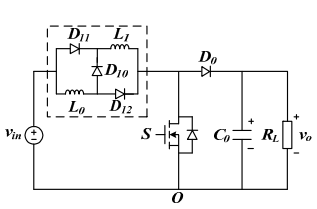

(a) Diode-inductor two-terminal cell.

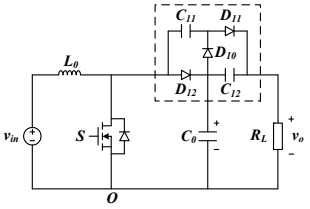

(c) Diode-capacitor three-terminal cell.

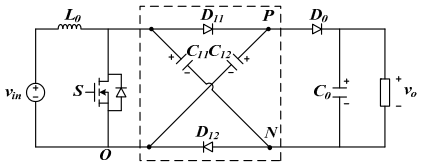

(e) Diode-capacitor four-terminal cell.

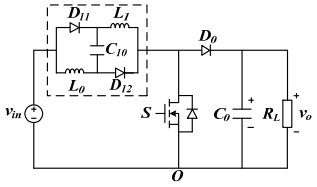

(b) Diode-inductor/capacitor two-terminal cell.

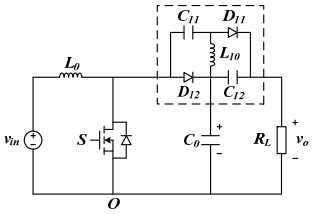

(d) Diode-capacitor/inductor three-terminal cell.

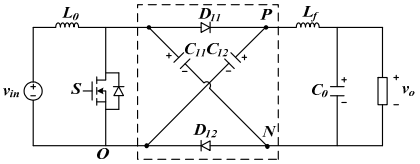

(f) Diode-capacitor/inductor four-terminal cell.

Fig.2 Boost derived high step-up DC-DC converter with basic diode-capacitor/inductor cell.

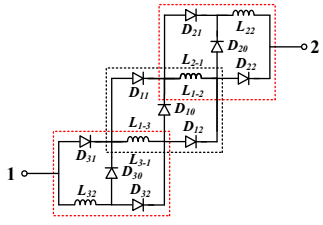

(a) Cascade connection.

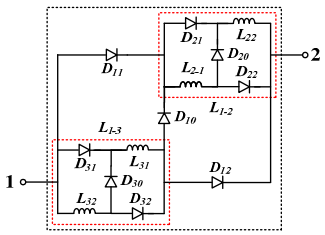

(b) Embedded connection.

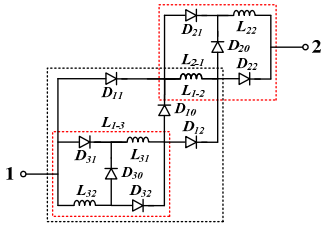

(c) Hybrid connection.

Fig.3 Multi-cell extension approaches with two-terminal diode-inductor cell (N=3).

same number of component and voltage boost capability. In steady state, every inductor current is almost constant and equals to each other. When the terminal-voltage v_{12} is positive, D_{11}, D_{12}, D_{21}, D_{22}, D_{31}, D_{32} are conducting, and current distribution is listed in Table.2. When v_{12} is negative, the current of D_{10}, D_{20}, D_{30} is i_L. Obviously, with embedded extension method, the diode conduction loss is minimum during $v_{12} \geq 0$ interval, which is 2/3 of cascade connection. Thus, it achieves high efficiency.

Table.2 Analysis of diode conduction current in multi-cell two-terminal diode-inductor network (N=3)

Terminal voltage	$v_{12} \geq 0$						
Derivation approach	D_{11}	D_{12}	D_{21}	D_{22}	D_{31}	D_{32}	Sum
Cascade connection	$2i_L$	$2i_L$	i_L	$3i_L$	$3i_L$	i_L	$12i_L$
Embedded connection	$2i_L$	$2i_L$	i_L	i_L	i_L	i_L	$8i_L$
Hybrid connection	$2i_L$	$2i_L$	i_L	$3i_L$	i_L	i_L	$10i_L$

For three/four-terminal diode-capacitor/inductor cell, the existing cascade extension method is the optimal one among different multi-cell connections.

III. Average Model of Dc-dc Converter with Multi-cell Capacitor/inductor Network

For high step-up DC-DC converter with multi-cell diode-capacitor/inductor network, the typical state space average modeling approach is not suitable directly. Evidently, it needs some modification. For simple analysis, it is assumed that all the capacitors and inductors in symmetrical multi-cell network have the same capacitance and inductance.

A. High step-up DC-DC Converter with two-terminal diode-inductor/capacitor network.

Fig.5 shows high step-up DC-DC converter with multi-cell two-terminal diode-inductor network. And Fig.6 shows two equivalent circuits according to the switching state of S.

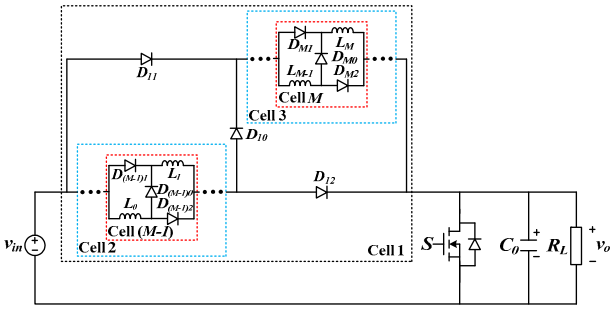

Fig.5 High step-up DC-DC converter with multi-cell two-terminal diode-inductor network.

During S=ON interval, DC source charges all the inductors in parallel connection, and transfer its electrostatic energy to magnetic energy. Taking all the inductor current and capacitor voltage as state variables, the state equation for this interval is:

$$\begin{cases} L_0 \dfrac{di_{L0}}{dt} = L_1 \dfrac{di_{L1}}{dt} = \ldots = L_{M-1} \dfrac{di_{L(M-1)}}{dt} = L_M \dfrac{di_{LM}}{dt} = v_{in} \\ C_0 \dfrac{dv_{C0}}{dt} = -\dfrac{v_{C0}}{R_L} \end{cases} \tag{1}$$

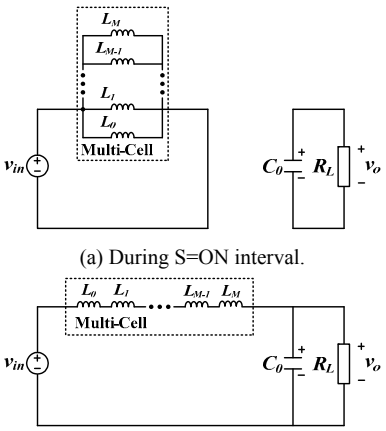

(a) During S=ON interval.

(b) During S=OFF interval.

Fig.6 The equivalent circuit of high step-up DC-DC converter with multi-cell diode-inductor network.

During S=OFF interval, DC source and all the inductors L_{11}, L_{12}, L_{21}, L_{22}…L_{N1}, L_{N1} are connected in series to charge C_0. The state equation for this interval is:

$$\begin{cases} L_0 \dfrac{di_{L0}}{dt} + L_1 \dfrac{di_{L1}}{dt} + \ldots + L_{(M-1)} \dfrac{di_{L(M-1)}}{dt} + L_M \dfrac{di_{LM}}{dt} = v_{in} - v_{C0} \\ C_0 \dfrac{dv_{C0}}{dt} = i_{L0} - \dfrac{v_{C0}}{R_L} \end{cases} \tag{2}$$

Obviously, every inductor has almost same current. Using state-space averaging method in one switching time period T_s, the average model can be obtained by $d\times(1)+(1-d)\times(2)$.

$$\begin{cases} (M+1)L_0 \dfrac{di_{L0}}{dt} = (1+Md)v_{in} - (1-d)v_{C0} \\ C_0 \dfrac{dv_{C0}}{dt} = (1-d)i_{L0} - \dfrac{v_{C0}}{R_L} \end{cases} \tag{3}$$

In this model, the control variable is d; the state variable to be controlled is i_{L0}, i_{L1}, … $i_{L(M-1)}$, i_{LM} and v_{C0}. The equilibrium operation point in steady state for given duty ratio $d=D$ is calculated by assuming the derivatives equal to zero.

$$\begin{cases} I_{L0} = I_{L1} = \ldots = I_{L(M-1)} = I_{LM} = \dfrac{V_{C0}}{(1-D)R_L} \\ V_{C0} = \dfrac{1+MD}{1-D} v_{in} \end{cases} \tag{4}$$

From (3), the equivalent circuit of average model is shown in Fig.7, in which $A=(1+Md)$, $L_e=(1+M)L_0$, $X=(1-d)$, $C_e=C_0$.

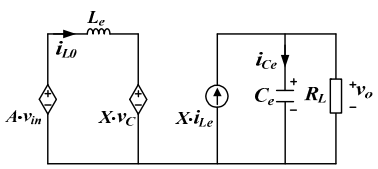

Fig.7 The average model of high step-up DC-DC converter with multi-cell two-terminal diode-inductor network.

Similarly, for high step-up DC-DC converter with multi-cell two-terminal diode-inductor/capacitor network shown in Fig.8. The state equations during S=ON and S=OFF interval can be written as (5) and (6), respectively.

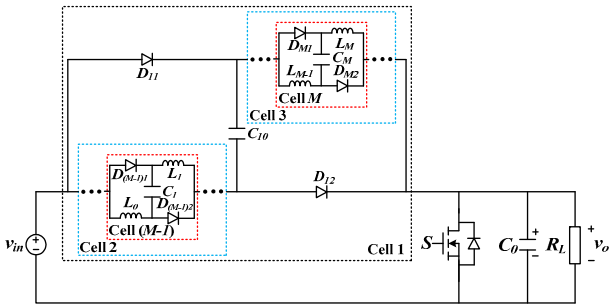

Fig.8 High step-up DC-DC converter with multi-cell two-terminal diode-inductor/capacitor network.

$$\begin{cases} L_0\dfrac{di_{L0}}{dt}=L_1\dfrac{di_{L1}}{dt}=\ldots=L_{M-1}\dfrac{di_{L(M-1)}}{dt}=L_M\dfrac{di_{LM}}{dt}=v_{in} \\ C_0\dfrac{dv_{C0}}{dt}=-\dfrac{v_{C0}}{R_L} \end{cases} \tag{5}$$

$$\begin{cases} \sum_{i=0}^{M}L_i\dfrac{di_{Li}}{dt}=v_{in}+v_{C1}+\ldots+v_{CM}-v_{C0} \\ C_0\dfrac{dv_{C0}}{dt}=i_{L0}-\dfrac{v_{C0}}{R_L} \end{cases} \tag{6}$$

Moreover, during *S*=ON interval, DC source charges every capacitor in diode-inductor/capacitor network through diodes. Assuming the capacitor voltage is almost constant in one switching time period, every capacitor meets:

$$v_{C1}=v_{C2}\ldots=v_{CM} \tag{7}$$

Using state-space averaging method and substituting (7) into (6), the reduced model is obtained by $d\times(5)+(1-d)\times(6)$.

$$\begin{cases} (M+1)L_0\dfrac{di_{L0}}{dt}=(1+M)v_{in}-(1-d)v_{C0} \\ C\dfrac{dv_{C0}}{dt}=(1-d)i_{L0}-\dfrac{v_{C0}}{R_L} \end{cases} \tag{8}$$

From (8), the equivalent circuit structure of average model for high voltage gain DC-DC converter with multi-cell two-terminal diode-capacitor/inductor network is the same as Fig.7, in which, $A=(1+M)$, $L_e=(1+M)L_0$, $X=(1-d)$, $C_e=C_0$.

B. High step-up DC-DCC Converter with four-terminal diode -capacitor network.

High step-up DC-DC converter with one-cell diode-capacitor network shown in Fig.2(f) is analyzed first. It has two operation modes according to the switching state of *S*. Using state space averaging method in one switching time period, the state equations can be obtained as:

$$\begin{cases} L_0\dfrac{di_{L0}}{dt}=v_{in}-(1-d)V_{C11} \\ 2C_{11}\dfrac{dv_{C11}}{dt}=(1-d)i_L-(1+d)i_{Lf} \\ L_f\dfrac{di_{Lf}}{dt}=(1+d)v_{C11}-v_{C0} \\ C_0\dfrac{dv_{C0}}{dt}=i_{Lf}-\dfrac{v_{C0}}{R_L} \end{cases} \tag{9}$$

From (9), using the controlled voltage/current source to reflect the relationship of DC transformer, the equivalent circuit of average model is show in Fig.9, in which $L_e=L_0$, $C_e=2C_{11}$, $X=(1-d)$, $Y=(1+d)$.

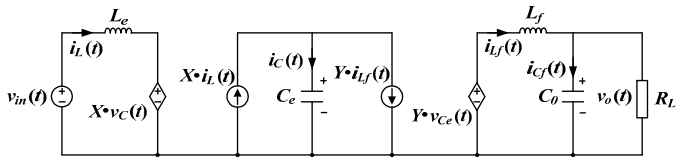

Fig.9 The average model of high step-up DC-DC converter with four-terminal diode-capacitor network and output *LC* filter.

As for high step-up DC-DC converter with multi-cell four-terminal diode-capacitor network and output *LC* filter shown in Fig.10, during *S*=ON interval, C_{11} and C_{12} are connected in series to charge C_{21} and C_{22}; C_{21} and C_{22} are connected in parallel. Due to symmetric network, each capacitor voltage in diode-capacitor network meets:

$$\begin{cases} v_{C11}=v_{C12}=v_C \\ v_{C21}=v_{C22}=2v_C \\ \vdots \\ v_{CN1}=v_{CN2}=Nv_C \end{cases} \tag{10}$$

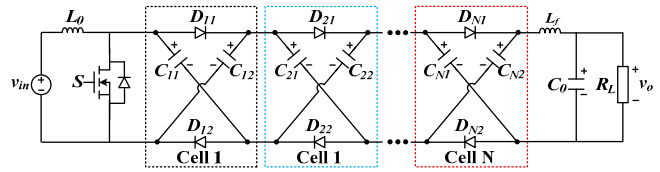

Fig.10 High step-up converter with multi-cell four-terminal diode-capacitor network and output *LC* filter.

Evidently, (10) is always satisfied without considering the change of duty ratio of *S*. The time constant of charge and discharge process for diode-capacitor network is much smaller than that of other components such as L_0 and *LC* filter. In diode-capacitor network, the voltage relationship of each capacitor is fixed and independent of duty ratio. Ignoring diode voltage drop and switching loss, multi-cell diode-capacitor network can be seemed as the ideal multi-stage DC transformer shown in Fig.11. According to the basic circuit theory, multi-stage DC transformers can be further simplified as single-stage transformer with capacitor. The transformer reflects voltage boost ratio and C_e reflects the stored energy in this multi-cell diode-capacitor network. C_E can be calculated by (11) according energy balance between multi-cell diode-capacitor network and single-stage DC transformer.

$$\frac{1}{2}\cdot C_e\cdot V_C^2=\sum_{i=1}^{N}\frac{1}{2}\cdot 2C_{11}\cdot V_{CN1}^2\Rightarrow C_e=\frac{N(N+1)(2N+1)}{3}C_{11} \tag{11}$$

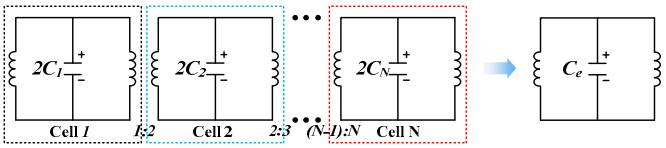

Fig.11 The equivalent circuit of multi-cell diode-capacitor network

After simplification, the average model equivalent circuit of high step-up DC-DC converter with multi-cell four-terminal

diode-capacitor network and *LC* filter is the same as Fig.9, in which L_e=L_0. Table 3 lists the key parameters for C_E and *Y*.

Table.3 Main parameters of the equivalent average model.

Cell Numbers (*N*)	Equivalent Capacitance (C_E)	*Y*(*d*,*N*)
1	$2C_{11}$	1+*d*
2	$10C_{11}$	3-*d*
…	…	…
N	$\frac{N(N+1)(2N+1)}{3}C_{11}$	$2\cdot \mathrm{int}(\frac{N}{2})+1+(-1)^{N+1}d$

Similarly, for high step-up DC-DC converter with multi-cell four-terminal diode-capacitor network and without output *LC* filter shown in Fig.12, multi-cell network and D_0, C_0 realize voltage multiplier. The voltage relationship between each capacitor is fixed and independent. Therefore, multi-cell diode-capacitor network are simplified and equivalently transferred to the output side according to energy balance.

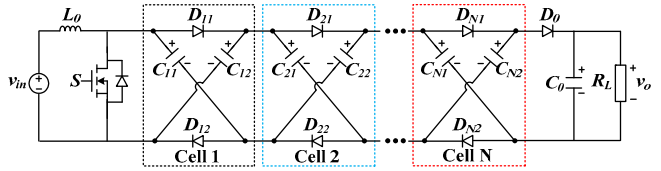

Fig.12 High step-up converter with multi-cell four-terminal diode-capacitor network.

$$\frac{1}{2}\cdot C_e\cdot\left[(N+1)V_C\right]^2=\sum_{i=1}^{N}\frac{1}{2}\cdot 2C_{i1}\cdot(i\cdot V_{Ci1})^2+\frac{1}{2}\cdot C_0\cdot\left[(N+1)V_C\right]^2$$
$$\Rightarrow C_e=\frac{N(2N+1)}{3(N+1)}C+C_0 \tag{12}$$

After simplification, using state-space averaging method the state equation of average model can be derived as

$$\begin{cases} L_0\dfrac{di_{L0}}{dt}=v_{in}-\dfrac{1-d}{N+1}v_{Ce} \\ C_e\dfrac{dv_{Ce}}{dt}=\dfrac{1-d}{N+1}i_{L0}-\dfrac{v_{Ce}}{R_L} \end{cases} \tag{13}$$

From (13), the equivalent circuit structure of average model for high step-up DC-DC converter with multi-cell four-terminal diode-capacitor network and without *LC* filter is the same as Fig.7, in which L_e=L_0, C_e=[N(2N+1)/3/(N+1)]C_{11}+C_0, A=1, X=(1-*d*)/(N+1), v_{Ce}= (N+1)/(1-*d*)v_{in}.

C. High step-up DC-DC Converter with three-terminal diode-capacitor/inductor network.

Fig.13 shows high step-up DC-DC converter with multi-cell three-terminal diode-capacitor network. During *S*=ON interval, D_{10}, D_{20}…D_{K0} are conducting. C_0 charges C_{11} through D_{10}, C_{12} charges C_{21} …ect. During S=OFF interval, D_{11}, D_{12}, D_{21}, D_{22}…D_{K1}, D_{K2} are conducting. C_{11}, C_{12} and C_{21}, C_{22} … and C_{N1}, C_{N2} are connected in parallel through conducting diode. Assuming capacitor voltage in one switching time period is almost constant, each capacitor always meets:

$$v_{C11}=v_{C12}=v_{C21}=v_{C22}...=v_{CK1}=v_{CK2} \tag{14}$$

With aforementioned simplification method, C_e of multi-cell diode-capacitor network including C_0 can be calculated according to energy balance, in which C_{i1}=C_{i2}=C_0.

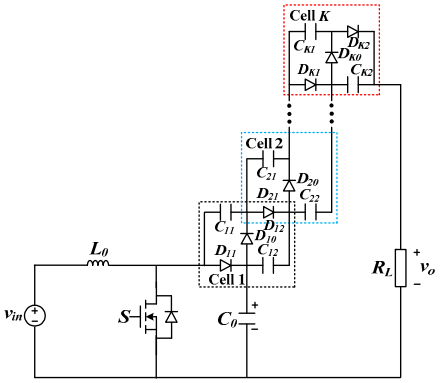

Fig.13 High step-up converter with multi-cell three-terminal diode-capacitor network.

$$\frac{1}{2}\cdot C_e\cdot\left[(K+1)V_C\right]^2=\frac{1}{2}C_0\cdot V_{C0}^2+\sum_{i=1}^{K}\frac{1}{2}\cdot 2C_{i1}\cdot V_{Ci1}^2$$
$$\Rightarrow C_e=\frac{2K+1}{(K+1)^2}C_{11} \tag{15}$$

After simplification, using state-space averaging method, the state equation of average model can be derived as

$$\begin{cases} L_0\dfrac{di_{L0}}{dt}=v_{in}-\dfrac{1-d}{1+K}v_{Ce} \\ C_e\dfrac{dv_{Ce}}{dt}=\dfrac{1-d}{1+K}i_{L0}-\dfrac{v_{Ce}}{R_L} \end{cases} \tag{16}$$

From (16), the average model of high step-up DC-DC converter with multi-cell three-terminal diode-capacitor network and without *LC* filter is the same as Fig.7, where L_e=L_0, C_e=(2K+1)/(K+1)^2C_{11}, A=1, X=(1-*d*)/(1+K), v_{Ce}=(1+K)/(1-*d*)v_{in}.

Fig.14 shows high step-up DC-DC converter with multi-cell three-terminal diode-capacitor/inductor network. Fig.15 shows two equivalent circuits during different switching state.

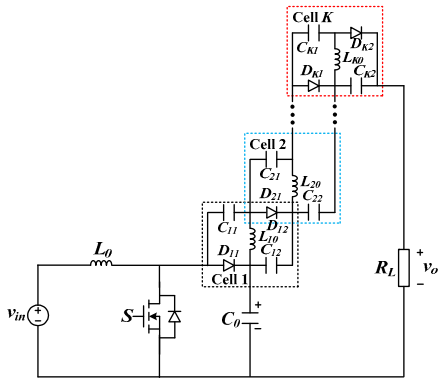

Fig.14 High step-up DC-DC converter with multi-cell three-terminal diode-capacitor/inductor network.

Form the equivalent circuits, the state equation during *S*=ON and *S*=OFF interval can be derived as (17) and (18).

Using state-space averaging method in one switching time period T_s, the average model can be obtained by *d*×(17)+(1-*d*)×(18). Moreover, due to symmetrical network and consistent parameters, it is assumed both capacitors in one cell have the same terminal voltage at the end of one switching time period.

$$\begin{cases} L_0\dfrac{di_{L0}}{dt}=V_{in} \\ C_0\dfrac{dv_{C0}}{dt}=-\sum_{i=1}^{K} i_{Li0}-\dfrac{v_{C0}+\sum_{i=1}^{K} v_{Ci2}}{R_L} \\ L_{i0}\dfrac{di_{Li0}}{dt}=v_{C0}-v_{Ci1} \\ C_{i1}\dfrac{dv_{Ci1}}{dt}=\sum_{j=i}^{K} i_{Lj0} \\ C_{i2}\dfrac{dv_{Ci2}}{dt}=-\sum_{j=i+1}^{K} i_{Lj0}-\dfrac{v_{C0}+\sum_{i=1}^{K} v_{Ci2}}{R_L} \end{cases} \quad (17)$$

$$\begin{cases} L_0\dfrac{di_{L0}}{dt}=V_{in}-v_{C0} \\ C_0\dfrac{dv_{C0}}{dt}=i_{L0}-\dfrac{v_{C0}+\sum_{i=1}^{K} v_{Ci2}}{R_L} \\ L_{i0}\dfrac{di_{Li0}}{dt}=-v_{Ci2} \\ C_{i1}\dfrac{dv_{Ci1}}{dt}+C_{i2}\dfrac{dv_{Ci2}}{dt}=i_{Li0}-\dfrac{v_{C0}+\sum_{i=1}^{K} v_{Ci2}}{R_L} \end{cases} \quad (18)$$

$$\begin{cases} L_0\dfrac{di_{L0}}{dt}=V_{in}-(1-d)v_{C0} \\ C_0\dfrac{dv_{C0}}{dt}=(1\text{-}d)i_{L0}-Kd\cdot i_{L10}-\dfrac{v_{C0}+Kv_{C11}}{R_L} \\ KL_{10}\dfrac{di_{L10}}{dt}=Kd\cdot v_{C0}-Kv_{C11} \\ 2\dfrac{C_{11}}{K}\dfrac{dKv_{C11}}{dt}=i_{Li0}-\dfrac{v_{C0}+Kv_{C11}}{R_L} \end{cases} \quad (19)$$

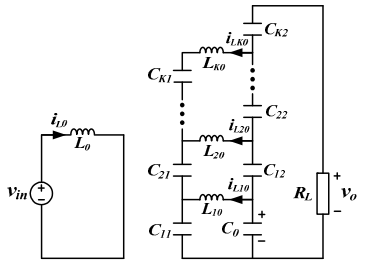

(a) During S=ON interval

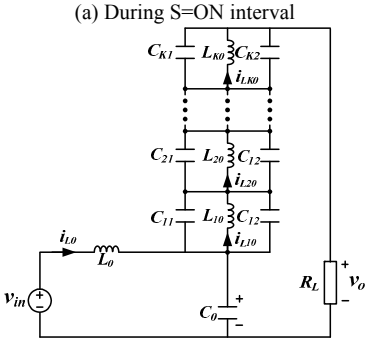

(b) During S=OFF interval

Fig.15 The equivalent circuit of high step-up DC-DC converter with multi-cell three-terminal diode-capacitor/inductor network.

The circuit structure of equivalent average model for high voltage gain DC-DC converter with multi-cell three-terminal diode-capacitor/inductor network is shown in Fig.16. in which L_e=KL_{10}, C_e=$2C_{11}/K$, v_{Ce}= Kv_{C11}.

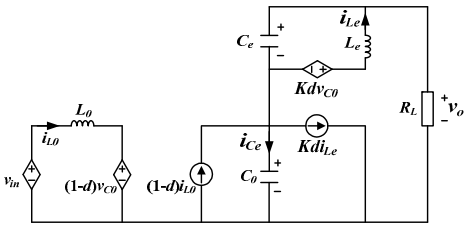

Fig.16 The average model of high step-up DC-DC converter with multi-cell three-terminal diode-capacitor/inductor network.

IV. Small Signal Model of DC-DC Converter with Multi-cell Capacitor/Inductor Network

Based on the reduced-order average model of high step-up DC-DC converters with different kinds of diode-capacitor/ inductor network in Section.III, performing small signal perturbation at given equilibrium point and ignoring the high-order infinitesimals, the small signal model and control-to-output transfer function can be derived easily. Table.4 lists the small signal model, transfer function and equivalent operation points of reduced two-order system model for high step-up DC-DC converters with two-terminal diode-inductor/capacitor cell, and three/four-terminal diode-capacitor without output *LC* filter. And Table.5 lists the small signal model and the equivalent operation points of reduced four-order system model for high step-up DC-DC converter with three/four-terminal diode-capacitor and output *LC* filter.

Table.4 Small signal model and transfer function of reduced two-order model for high step-up DC-DC converters with multi-cell diode-capacitor/inductor network.

High step-up DC-DC converter	Two-terminal diode-inductor cell	Two-terminal diode-inductor/capacitor cell	Four-terminal diode-capacitor cell without *LC* filer/Three-terminal diode-capacitor cell
Small signal model	$\begin{cases}(M+1)L_0\dfrac{d\hat{i}_{L0}}{dt}=(MV_{in}+V_{C0})\hat{d}-(1-D)\hat{v}_{C0}\\ C_0\dfrac{d\hat{v}_{C0}}{dt}=(1-D)\hat{i}_{L0}-I_{L0}\hat{d}-\dfrac{\hat{v}_{C0}}{R_L}\end{cases}$	$\begin{cases}(M+1)L_0\dfrac{d\hat{i}_{L0}}{dt}=V_{C0}\hat{d}-(1-D)\hat{v}_{C0}\\ C_0\dfrac{d\hat{v}_{C0}}{dt}=(1-D)\hat{i}_{L0}-I_{L0}\hat{d}-\dfrac{\hat{v}_{C0}}{R_L}\end{cases}$	$\begin{cases}(1+N)L_0\dfrac{d\hat{i}_{L0}}{dt}=V_{Ce}\hat{d}-(1-D)\hat{v}_{Ce}\\ (1+N)C_e\dfrac{d\hat{v}_{Ce}}{dt}=(1-D)\hat{i}_{L0}-I_{L0}\hat{d}-\dfrac{\hat{v}_{Ce}}{R_L}\end{cases}$
Transfer function	$\begin{cases}\dfrac{\hat{i}_L}{\hat{d}}=\dfrac{(MV_{in}+V_{C0})C_0\cdot s+\dfrac{MV_{in}+V_{C0}}{R_L}+I_L(1-D)}{(M+1)LC_0\cdot s^2+(M+1)\dfrac{L}{R_L}\cdot s+(1-D)^2}\\ \dfrac{\hat{v}_C}{\hat{d}}=\dfrac{-(1+M)I_{L0}L_0\cdot s+(1-D)(MV_{in}+V_{C0})}{(M+1)LC_0\cdot s^2+(M+1)\dfrac{L}{R_L}\cdot s+(1-D)^2}\end{cases}$	$\begin{cases}\dfrac{\hat{i}_L}{\hat{d}}=\dfrac{C_0V_{C0}\cdot s+\dfrac{V_{C0}}{R_L}+I_L(1-D)}{(M+1)LC_0\cdot s^2+(M+1)\dfrac{L}{R_L}\cdot s+(1-D)^2}\\ \dfrac{\hat{v}_C}{\hat{d}}=\dfrac{-(1+M)I_{L0}L_0\cdot s+(1-D)V_{C0}}{(M+1)LC_0\cdot s^2+(M+1)\dfrac{L}{R_L}\cdot s+(1-D)^2}\end{cases}$	$\begin{cases}\dfrac{\hat{i}_L}{\hat{d}}=\dfrac{(N+1)C_eV_{Ce}\cdot s+\dfrac{V_{Ce}}{R_L}+I_{L0}(1-D)}{(N+1)L_0C_0\cdot s^2+(M+1)\dfrac{L_0}{R_L}\cdot s+(1-D)^2}\\ \dfrac{\hat{v}_C}{\hat{d}}=\dfrac{-(N+1)I_{L0}L_0\cdot s+(1-D)V_{C0}}{(N+1)^2L_0C_e\cdot s^2+(N+1)\dfrac{L_0}{R_L}\cdot s+(1-D)^2}\end{cases}$
The equivalent operation points	$V_{C0}=\dfrac{1+Md}{1-D}v_{in}, I_{L0}=\dfrac{1+Md}{(1-D)^2}\dfrac{v_{in}}{R_L}$	$V_{C0}=\dfrac{1+M}{1-D}v_{in}, I_{L0}=\dfrac{1+M}{(1-D)^2}\dfrac{v_{in}}{R_L}$	$V_{Ce}=\dfrac{1+N}{1-D}v_{in}, I_{L0}=\dfrac{(1+N)^2}{(1-D)^2}\dfrac{v_{in}}{R_L}$

Table.5 Small signal model of reduced four-order model for high step-up DC-DC converters with multi-cell diode-capacitor/inductor network.

High step-up DC-DC converter	Four-terminal diode-capacitor cell with *LC* filter	Three-terminal diode-capacitor/inductor cell
Small signal model	$\begin{cases} L_0\frac{d\hat{i}_{L0}}{dt}=-(1-D)\hat{v}_{C11}+V_{C11}\hat{d} \\ 2C_{11}\frac{d\hat{v}_{C11}}{dt}=(1-D)\hat{i}_L-I_L\hat{d}-Y(N,D)\hat{i}_{Lf}-I_{Lf}\hat{d} \\ L_f\frac{d\hat{i}_{Lf}}{dt}=Y(N,D)\hat{v}_{C11}+V_{C11}\hat{d}-\hat{v}_{C0} \\ C_0\frac{d\hat{v}_{C0}}{dt}=\hat{i}_{Lf}-\frac{\hat{v}_{C0}}{R_L} \end{cases}$	$\begin{cases} L_0\frac{d\hat{i}_{L0}}{dt}=-(1-D)\hat{v}_{C0}+V_{C0}\hat{d} \\ C_0\frac{d\hat{v}_{C0}}{dt}=(1-D)\hat{i}_{L0}-I_{L0}\hat{d}-KD\hat{i}_{Le}-KI_{Le}\hat{d}-\frac{\hat{v}_{C0}+\hat{v}_{Ce}}{R_L} \\ L_e\frac{d\hat{i}_{Le}}{dt}=KD\hat{v}_{C0}+V_{C0}\hat{d}-\hat{v}_{Ce} \\ C_e\frac{d\hat{v}_{Ce}}{dt}=\hat{i}_{Le}-\frac{\hat{v}_{C0}+\hat{v}_{Ce}}{R_L} \end{cases}$
The equivalent operation points	$V_{Ce}=\frac{Y(N,D)}{1-D}v_{in}, I_{Le}=\frac{Y^2(N,D)}{(1-D)^2}\frac{v_{in}}{R_L}$, $I_{Lf}=\frac{Y(N,D)}{(1-D)}\frac{v_{in}}{R_L}, V_{Co}=\frac{Y(N,D)}{1-D}v_{in}$.	$I_{L0}=\frac{(1+KD)^2}{(1-D)^2}\frac{v_{in}}{R_L}, V_{C0}=\frac{1}{1-D}v_{in}$, $I_{Le}=\frac{1+KD}{1-D}\frac{v_{in}}{R_L}, V_{Ce}=\frac{KD}{1-D}\frac{v_{in}}{R_L}$.

V. Simulation and Experiment Verification

Numerical simulations using MATLAB/Simulink have been performed to verify the aforementioned reduced-order modeling approach and the theoretical analysis. Fig.17 shows waveforms of high step-up DC-DC converter with two-cell four-terminal diode-capacitor network and *LC* filter in time domain for the step-up of duty ratio from *0.5* to *0.7* at *t=0.2s* and step-down at t=*0.9s*. The main circuit parameters are: L_0=*5mH;* C_{11}=*50uF;* L_f=*10mH;* C_f=*500uF;* V_{in}=*60V;* f_s=*10kHz*. The dynamic response of inductor current and output voltage for the reduced four-order model are almost consist with the original real circuit with two cells diode-capacitor network.

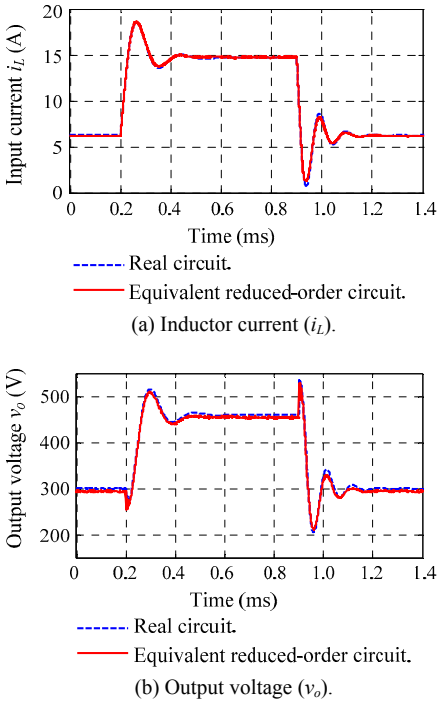

Fig.17 Time-domain waveforms of high step-up DC-DC converter with two-cell four-terminal diode-capacitor network and *LC* filter.

Fig.18 shows the corresponding frequency characteristic of high step-up DC-DC converter with four-terminal diode-capacitor network and *LC* filter.

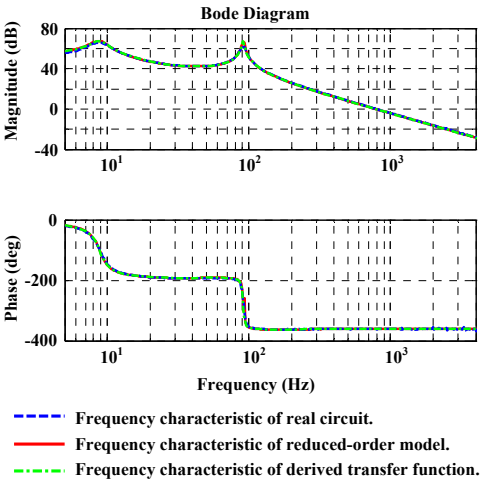

Fig.18 Frequency characteristic of high step-up DC-DC converter with two-cell four-terminal diode-capacitor network and *LC* filter.

Fig.19 shows the frequency characteristic of high step-up DC-DC converter with three-terminal diode-capacitor network. The simulation results and theoretical calculation value are almost consistent with each other during low frequency range.

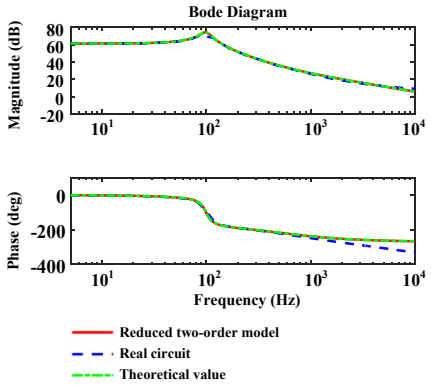

Fig.19 Frequency characteristic of high step-up DC-DC converter with two-cell three-terminal diode-capacitor network.

A laboratory prototype was built to verify the proposed modeling approach and closed-loop controller design. The specification of the prototype are V_{in}=48V; *L*=1mH; *C*=50uF; L_f=5mH; C_f=500uF; R_L=140Ω; f_s=10kHz, N=2.

Fig.20 shows the measured frequency characteristic for high step-up DC-DC converter with two-cell diode-capacitor network and *LC* filter.

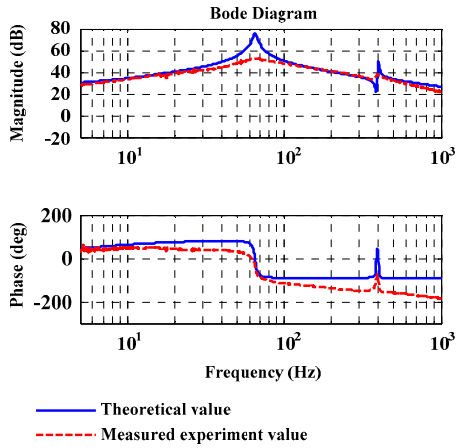

(a) Duty ratio to boost inductor current $G_{iL\_d}(s)$.

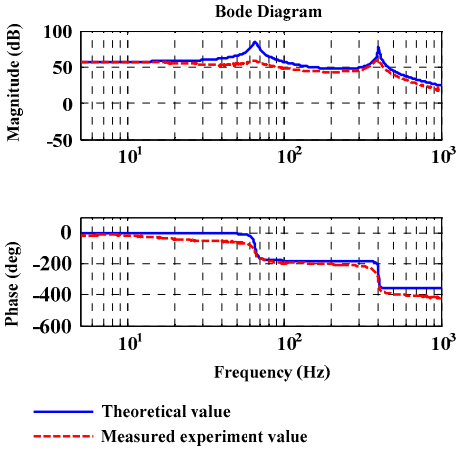

(b) Duty ratio to output capacitor voltage $G_{vo\_d}(s)$.

Fig.20. Bode diagram of duty ratio to capacitor voltage $G_{vo\_d}(s)$ for high voltage gain DC-DC converter with two-cell four-terminal diode-capacitor network and *LC* filter.

The simulations and experiments prove the validity of the reduced-order modeling approach, which are suitable for high step-up DC-DC converter with multi-cells diode-capacitor/ inductor network.

VI. Conclusion

Reduced-order modeling approaches are one of the main challenges for step-up DC-DC converter with multi-cell diode-capacitor/inductor network. Transient modeling analysis reveals that time constant of each component in diode-capacitor/inductor network is much smaller than that of other circuit if the directly charging and discharge processes between capacitor through diode is fast enough. The voltage/ current relationship of each capacitor/inductor in multi-cell network is fixed. Multi-cell diode-capacitor/inductor network can be seemed as multi-stage DC transformer. Based on the unique feature, this paper proposes the reduced-order modeling approach, which is suitable for high step-up DC-DC converter with multi-cell diode-capacitor/inductor network. The unified reduced-order model contributes to better understanding of circuit characteristic and guide for linear controller parameters design. The simulations and experiments prove the validity of theoretical analysis and reduced-order modeling approach.

References

[1] W. Li and X. He, "Review of nonisolated high-step-up dc/dc converters in photovoltaic grid-connected applications", IEEE Trans. Ind. Electron., vol. 58, no. 4, pp. 1239–1250, Apr. 2011.

[2] Abutbul O, Gherlitz A and Berkovich Y, "Step-up switching-mode converter with high voltage gain using a switched-capacitor circuit," IEEE Trans. Circuit and System, vol. 50, no.8, pp. 1098–1102, 2003.

[3] H. Nomura, K. Fujiwara, and M. Yoshida, "A new dc–dc converter circuit with larger step-up/down ratio," in Proc. IEEE Power Electron. Spec. Conf., 2006, pp. 3006–3012.

[4] E. H. Ismail, M. A. AI-Saffar, A. J. Sabzali, and A. A. Fardoun, "A family of single-switch PWM converters with high voltage-boosting conversion ratio," IEEE Trans. Circuits Syst. I, Reg. Papers, vol. 55, no. 4, pp. 1159–1171, May 2008.

[5] B. Axelrod, Y. Berkovich, and A. Ioinovici, "Switched-capacitor/switched-inductor structures for getting transformerless hybrid DC-DC PWM converters," IEEE Trans. Circuits Syst. I, Reg. Papers, vol. 55, no. 2, pp. 687–696, Mar. 2008.

[6] Yan Zhang, Jinjun Liu, "Comparison of Conventional DC-DC Converter and a Family of Diode-Assisted DC-DC Converter in Renewable Energy Applications," Journal of Power Electronics, vol. 14, no.2, pp. 203-216, March 2014.

[7] J.-H. Kim, D.-Y. Jung, S.-H. Park, and S.-W. Lee, "High efficiency soft-switching boost converter using a single switch," Journal of Power Electronics, vol. 9, pp. 929-939, Nov. 2009.

[8] J. Calvente, L. Martinez-Salamero, P. Garces and A. Romero, "Zero dynamics-based design of damping networks for switching converters", IEEE Trans. Aerosp. Electron. Syst., vol. 39, no. 4, pp.1292-1303, Oct. 2003.

[9] J.-H. Kim, D.-Y. Jung, S.-H. Park, and S.-W. Lee, "High efficiency soft-switching boost converter using a single switch," Journal of Power Electronics, vol. 9, pp. 929-939, Nov. 2009.

[10] K. Yao, Y. Mao, X. Ming, and F. C. Lee, "Tapped-inductor buck converter for high-step-down DC-DC conversion," IEEE Trans. Power Electron., vol. 20, no.1 pp. 775-780, July. 2005.

[11] J. Calvente, L. Martinez-Salamero, P. Garces and A. Romero, "Zero dynamics-based design of damping networks for switching converters", IEEE Trans. Aerosp. Electron. Syst., vol. 39, no. 4, pp.1292-1303, Oct. 2003.

[12] J. Calvente, L. Martinez-Salamero, H. Valderrama and E. Vidal-Idiarte, "Using magnetic coupling to eliminate right half-plane zeros in boost converters", IEEE Power Electron Lett., vol. 2, no. 2, pp.58-62, June. 2004.

[13] Yu Gu, Donglai Zhang and Zhongyanng Zhao, "Input/Output current ripple cancellation and RHP zero elimination in a boost converter using an integrated magnetic technique", IEEE Trans. Power Electron., vol. 30, no. 2, pp.747-756, Feb. 2015.

[14] Santanu Kapat, Amit Patra and Soumitro Banerjee, "A current-controlled tristate boost converter with improved performance through RHP zero elimination", IEEE Trans. Power Electron., vol. 24, no. 3, pp.776-786, March. 2009.

[15] Rajeev Singh and Santanu Mishra "A Magnetically Coupled Feedback-Clamped Optimal Bi-directional Battery Charger", IEEE Trans. On Ind. Electronics, vol. 60, no. 2, pp. 422-432, Feb. 2013.